Permeation of Protons, Potassium Ions, and Small Polar Molecules Through Phospholipid Bilayers as a Function of Membrane Thickness

S. Paula,* A. G. Volkov,* A. N. Van Hoek,‡ T. H. Haines,§ and D. W. Deamer*
*Department of Chemistry and Biochemistry, University of California, Santa Cruz, California 95064; ‡Cardiovascular Research Institute, University of California, San Francisco, California 94143; and §Department of Chemistry, CUNY, New York, New York 10031 USA

ABSTRACT Two mechanisms have been proposed to account for solute permeation of lipid bilayers. Partitioning into the hydrophobic phase of the bilayer, followed by diffusion, is accepted by many for the permeation of water and other small neutral solutes, but transient pores have also been proposed to account for both water and ionic solute permeation. These two mechanisms make distinctively different predictions about the permeability coefficient as a function of bilayer thickness. Whereas the solubility-diffusion mechanism predicts only a modest variation related to bilayer thickness, the pore model predicts an exponential relationship. To test these models, we measured the permeability of phospholipid bilayers to protons, potassium ions, water, urea, and glycerol. Bilayers were prepared as liposomes, and thickness was varied systematically by using unsaturated lipids with chain lengths ranging from 14 to 24 carbon atoms. The permeability coefficient of water and neutral polar solutes displayed a modest dependence on bilayer thickness, with an approximately linear fivefold decrease as the carbon number varied from 14 to 24 atoms. In contrast, the permeability to protons and potassium ions decreased sharply by two orders of magnitude between 14 and 18 carbon atoms, and leveled off, when the chain length was further extended to 24 carbon atoms. The results for water and the neutral permeating solutes are best explained by the solubility-diffusion mechanism. The results for protons and potassium ions in shorter-chain lipids are consistent with the transient pore model, but better fit the theoretical line predicted by the solubility-diffusion model at longer chain lengths.

INTRODUCTION

The balance between maintenance and dissipation of concentration gradients across cell membranes is crucial for the function of biological systems. Processes such as oxidative and photosynthetic phosphorylation require membranes that provide effective barriers to passive diffusion of protons. In other cases, the rapid exchange of molecules such as water across a cell membrane is essential, so that water channel proteins are required to increase the intrinsic water permeability of the membrane. Permeability coefficients of many ions and small neutral molecules have been determined experimentally and vary over a remarkably broad range. Despite the availability of these data, the mechanism of passive permeation is still not completely understood.

In the past, permeability coefficients characterizing the lipid bilayer as a barrier to permeation have been calculated from solubility-diffusion theory (Finkelstein, 1987), which is the most generally accepted description of water permeability of bilayers to date. This approach treats the membrane as a thin static slab of hydrophobic matter embedded in an aqueous environment. To cross the membrane, the permeating particle must dissolve in the hydrophobic region, diffuse across, and leave by redissolving into the second aqueous phase. If the membrane thickness and the diffusion and partition coefficients of the permeating species are known, the permeability coefficient can be calculated. The partition coefficients for small neutral molecules are usually determined by experiment (for references see Finkelstein, 1987), whereas partition coefficients for ions can be derived from the Born energy, the energy required to transfer a charged particle from the high dielectric aqueous phase to the low dielectric membrane interior (Parsegian, 1969; Dilger et al., 1979). In many cases, however, discrepancies between predicted and measured permeabilities have raised questions about this approach. For example, the observed permeability of sodium ions exceeds the calculated value by three orders of magnitude (Hauser et al., 1973). Proton permeation rates were found to be even larger, five to six orders of magnitude above the values expected from comparisons with other monovalent cations (Deamer and Nichols, 1989). Several attempts have been made to account for these discrepancies. Hydrophobic and image energies have been added to the Born energy term, yielding a smaller net energy of transfer and thus increasing the predicted permeability. It has also been suggested that the hydrated radii can be used instead of the bare ionic radii, which leads to lower translocation energies and therefore higher permeation rates (Deamer and Volkov, 1995).

An alternative mechanism to the solubility-diffusion description has been proposed, which suggests that permeation across a bilayer membrane occurs through hydrated transient defects produced by thermal fluctuations (Nagle and Scott, 1978; Nichols and Deamer, 1980; Elamrani and Blume, 1983; Lawaczeck, 1988; Jansen and Blume, 1995). By passing through pores, the permeating particle can avoid the Born energy barrier associated with the solubility-diffusion mechanism. Furthermore, protons can be translo-

Received for publication 12 June 1995 and in final form 9 October 1995.
Address reprint requests to Dr. Stefan Paula, Department of Chemistry and Biochemistry, University of California at Santa Cruz, Santa Cruz, CA 95064. Tel.: 408-459-5157; Fax: 408-459-5158; E-mail: stefan@chemistry.ucsc.edu.

0006-3495/96/01/339/10 $2.00

cated by a Grotthus-type mechanism along water "wires" spanning the membrane in such defects. Because this process is intrinsically much faster than diffusion, the transient pore model can also account for the high permeability observed for protons.

In an attempt to understand the underlying mechanism of solute permeation, this study presents an investigation of the effect of bilayer thickness on the permeability of several solutes. Bilayer thickness was varied by using phosphatidylcholines with fatty acid chain lengths ranging from 14 to 24 carbon atoms and containing *cis* double bonds. The permeabilities of phospholipid bilayers to protons, potassium ions, water, urea, and glycerol were measured at 30°C. The influence of membrane thickness on the permeability coefficient was compared to predictions made by the two models described above. According to the pore model, transient defects should become significantly less common as bilayer thickness increases, leading to a pronounced drop in permeability. The solubility-diffusion model, however, predicts a much smaller effect of bilayer thickness on permeability and differentiates clearly between charged and uncharged permeating particles. In principle it should be possible to distinguish between these two mechanisms by exploring the effect of membrane thickness on the permeation rates of various solutes.

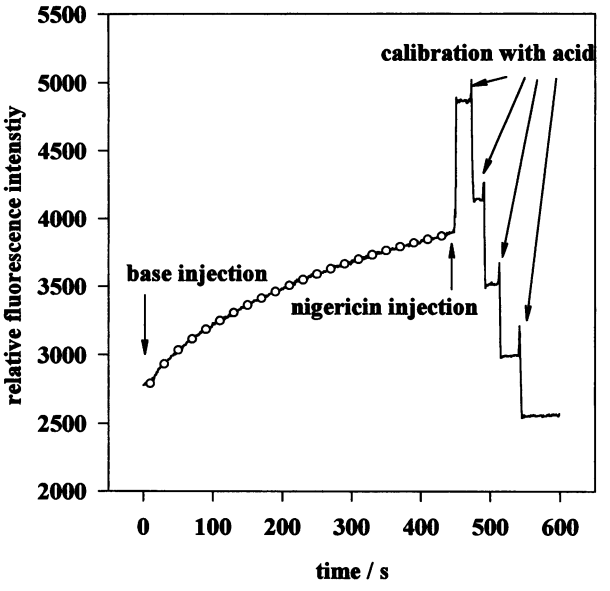

FIGURE 1 Time course of fluorescence of pyranine (0.5 mM) trapped in liposomes (0.5 mg/ml) in response to a pH-gradient induced by the addition of 7.5 μl 1 M KOH (initial pH: 6.75; final pH: 7.25; T = 30°C). Liposomes were made of dipalmitoleoyl-PC in 50 mM K_2SO_4, 10 mM ACES, MES, TES, and Tricine each. The symbols (○) show a double-exponential fit to the data. Nigericin was added to equilibrate the pH inside and outside the liposomes. Four 2-μl aliquots of 0.5 M H_2SO_4 were added to calibrate the system.

MATERIALS AND METHODS

Chemicals

All phospholipids were obtained from Avanti Biochemicals (Birmingham, AL). The fluorescent dye pyranine (8-hydroxy-1,3,6-pyrenetrisulfonate) was purchased from Eastman Kodak (Rochester, NY). Sulfuric acid, glycerol, and chloroform were from Fisher (Pittsburgh, PA), and urea was from MCB (Norwood, OH). All other chemicals were obtained from Sigma (St. Louis, MO). Deionized water for making buffer solutions was prepared with a Barnstead (Boston, MA) Water-I ultrapurification device.

Measurement of proton permeation

Unilamellar vesicles were prepared by extrusion of phosphatidylcholines with monounsaturated fatty acids composed of 14 to 24 carbon atoms with *cis* double bonds located at the chain center. A chloroform solution containing 10 mg of lipid was dried by a gentle stream of nitrogen and then kept under vacuum for at least 2 h. Under an argon atmosphere, the lipid was then hydrated in 1 ml of the appropriate buffer (pH 6.75 for basic jumps and pH 7.25 for acidic jumps, adjusted with potassium hydroxide), containing 50 mM potassium sulfate, 0.5 mM pyranine, and 10 mM each of *N*-[2-acetamido]-2-aminoethanesulfonic acid (ACES), 2-[*N*-morpholino]ethanesulfonic acid (MES), *N*-Tris[hydroxymethyl]methyl-2-aminoethanesulfonic acid (TES), and *N*-Tris[hydroxymethyl]methylglycine (Tricine). This buffer mixture displayed a constant buffer capacity over the entire pH range of interest. The suspension was vortexed briefly and extruded at least ten times through a polycarbonate filter (Nucleopore, Costar Corp.), which had a pore diameter of 200 nm. Pyranine in the external phase of the vesicle dispersion was removed by passing the sample through a Sephadex G-50 column (0.5 cm^2 × 15 cm). Size distribution and mean hydrodynamic radius of the vesicles were determined by quasi-elastic light scattering with a BI-90 analyzer (Brookhaven Instruments Corp., Holtsville, NY).

Pyranine fluorescence, indicating the intravesicular pH (Clement and Gould, 1981; Grzesiek and Dencher, 1986), was monitored with a SLM 8000 C spectrofluorimeter (SLM Instruments, IL) at an excitation wavelength of 430 nm; the emission was recorded at 515 nm. Samples contained 1.5 ml of approximately 0.5 mM lipid dispersion and were stirred continuously in a thermostated (Haake FJ, Berlin) holder at 30°C. At this temperature, all lipids were in the liquid-crystalline phase. Two microliters of a 100 μM valinomycin in ethanol solution was added to the sample before starting the experiment to dissipate any diffusion potential across the membrane. pH jumps (0.5 pH units in each direction) were induced by adding 7.5 μl of concentrated sulfuric acid (0.5 M) or potassium hydroxide solution (1 M), respectively. The initial pH was 7.25 for acidic jumps and 6.75 for basic jumps. After recording the fluorescence change in response to the pH change, 1 μl nigericin (100 μM) in ethanol was added to equilibrate the pH across the vesicle membrane. Calibrations to determine the relationship between fluorescence and the amount of added protons or hydroxide ions were performed by injecting several well-defined amounts of acid or base. Fig. 1 shows the time course of a typical experiment.

The fluorescence curve was fitted by two exponentials, which described the experimental data better than one exponential because pyranine fluorescence was not an exact linear function of pH. The initial slope was obtained from the first derivative with respect to time. The net proton flux J was calculated from the following equation:

$$J = \frac{\mathrm{d}\,FU}{\mathrm{d}t} \cdot \frac{B \cdot V}{A} = \frac{\mathrm{d}\,FU}{\mathrm{d}t} \cdot \frac{B \cdot r}{3}. \qquad (1)$$

B links the change in fluorescence to the amount of added protons or hydroxide ions. For spherical liposomes of narrow size distribution, the ratio of the vesicle surface area, A, to the vesicle volume, V, could be expressed in terms of the liposome mean radius, r. For all liposome samples, the observed mean diameters as measured corresponded (200 nm ± 10%) to the diameter of the polycarbonate filters, and the size distribution was narrow.

Dividing the flux J by the proton concentration gradient Δc across the bilayer yielded the permeability coefficient P:

$$P = J/\Delta c. \qquad (2)$$

Δc was determined from the change in pH of the sample prior to and after the pH jump. pH values were measured with an Accumet 925 MP pH meter (Fisher, NY) and a combination pH electrode. The calculations assumed that only protons were transported during discharge of the pH gradient.

Measurement of potassium ion permeation

To determine potassium ion permeabilities, the efflux of potassium ions out of liposomes was measured with a cation-selective electrode (Beckman) (Barchfeld and Deamer, 1988). This electrode was used in combination with an Accumet 925 MP pH meter (Fisher, NY) and a Ag/AgCl reference electrode (Corning). To avoid sample contaminations by potassium ions, the saturated potassium chloride solution in the outer chamber of the reference electrode was replaced by a saturated choline chloride solution. Calibration of the electrodes was achieved by measuring the electrode output for several potassium sulfate standard solutions prepared in 20 mM HEPES/choline hydroxide and 300 mM choline chloride, pH 8, covering the concentration range between 20 μM and 0.2 M.

Liposome samples (approximately 10 mg/ml) were prepared by the extrusion method in 200 mM potassium sulfate and 20 mM HEPES/potassium hydroxide, pH 8. Gel filtration through a Sephadex G-50 column (0.5 $cm^2 \times 10$ cm) was used to replace the external volume of the liposome dispersion by isoosmotic 300 mM choline chloride in 20 mM HEPES/choline hydroxide (pH 8). Immediately after the filtration step, the samples (2 ml) were placed into a sample holder thermostated at 30°C with a water bath, and the time course of the voltage output of the immersed electrodes was registered by a chart recorder (Microscribe 4500, Houston Instruments) connected to a pH meter. Continuous sample mixing was achieved by gently bubbling nitrogen through the sample. Fig. 2 presents a typical voltage-time trace.

For the flux determination, the initial change of voltage per second was converted into a change of potassium ion concentration per second, $\Delta K^+/\Delta t$. Because potassium ion efflux was slow, the time delay between putting the sample on the column and getting a stable reading of the electrodes (5–8 min), did not affect the measurement. Permeabilities were calculated according to the following equation:

$$P = \frac{\Delta [K^+] \cdot V}{\Delta t \cdot A \cdot \Delta c} \tag{3}$$

where V was the external volume of the liposome dispersion and equaled the volume of the sample, if the small liposome volume was neglected. A was the total surface area of the liposomes and was obtained by assaying the lipid concentration (Ames, 1966) and assuming a headgroup area of 0.7 nm^2 per lipid molecule (Small, 1967).

To test whether the potassium ion efflux was limited by the influx of charge-compensating protons, test experiments were performed in the presence of the protonophore carbonyl-cyanide-*m*-chlorophenylhydrazone (CCCP) (0.2 μM). Because no effect on the kinetics of potassium ion efflux could be detected, it was concluded that potassium ion permeation was not hindered by electrostatic diffusion potentials.

Measurement of water, glycerol, and urea permeation

The osmotic water permeability coefficient (P_f) of phospholipid bilayers was determined from the kinetics of liposome volume change induced by an imposed transmembrane osmotic gradient, as described previously (Van Heeswijk and van Os, 1986; Verkman et al., 1985; Ye and Verkman, 1989; De Gier, 1993). Measurements were performed on a Hi-Tech SF51 stopped-flow apparatus (Wiltshire, England) with a dead time of ~1.5 ms and a mixing efficiency of more than 99% within 1 ms. Scattered light (520 nm) at 90° was recorded at three sequential time scales. At 30°C, 75 μl of a liposome sample prepared by the extrusion method (approximately 0.5 mg/ml lipid in 5 mM each ACES, MES, TES, TRICINE and 50 mM potassium sulfate, pH 7) was mixed with an equal volume of the same buffer containing 200 mM sucrose, 400 mM glycerol, or 400 mM urea.

A typical time course of the scattered light intensity that could be resolved in two stages (if urea or glycerol was the solute) is shown in Fig. 3. The fast initial increase of the light scattering signal was caused by the shrinking of the liposomes as water responded to the osmotic gradient. This process was followed by a slower recovery of the signal to its initial value, which corresponded to the influx of the external solute and its concomitant water (Cohen and Bangham, 1971). If sucrose was used as solute, the second process was too slow to be resolved on the established time scale and the data points were fit to a single exponential decay (Verkman et al., 1985; van Heeswijk and van Os, 1986). If urea or glycerol was the solute, the entire curve was fit to the sum of two exponentials with opposite signs. For the calculation of the osmotic water permeability coefficient, P_f, the rate constant of the initial, fast process was used according to the following equation:

$$P_f = \frac{k \cdot A}{V_w \cdot V_o \cdot \Delta c} = \frac{k \cdot r}{3 \cdot V_w \cdot \Delta c}. \tag{4}$$

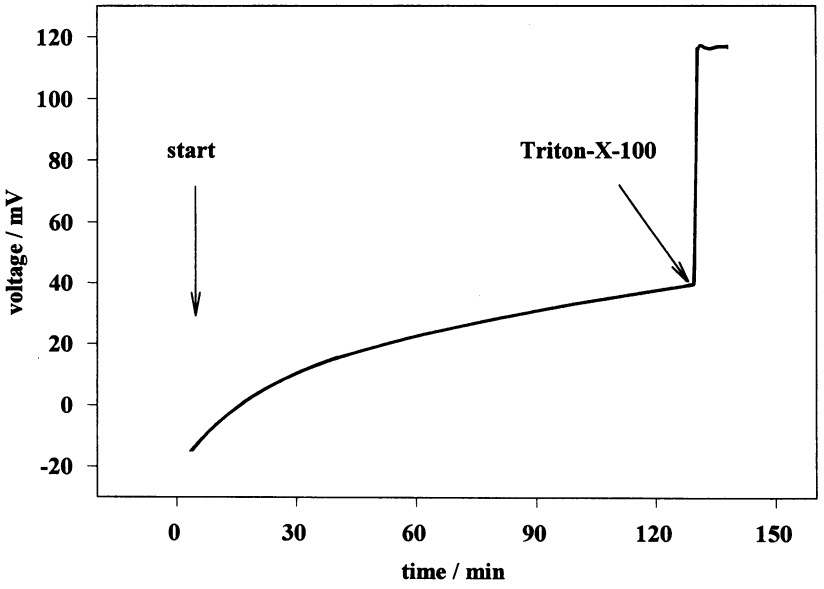

FIGURE 2 Time course of voltage output of a potassium ion-sensitive electrode, detecting the potassium ion escape from dipalmitoleoyl-PC liposomes. The internal buffer contained 0.2 M K_2SO_4, 20 mM HEPES/choline hydroxide at pH 8, and the external buffer contained 0.3 M choline chloride, 20 mM HEPES/choline hydroxide at pH 8. Potassium ion concentrations inside and outside the liposomes were equilibrated at the end of the experiment by adding 200 μl 200 mM Triton X-100 solution, which dissolved the liposomes.

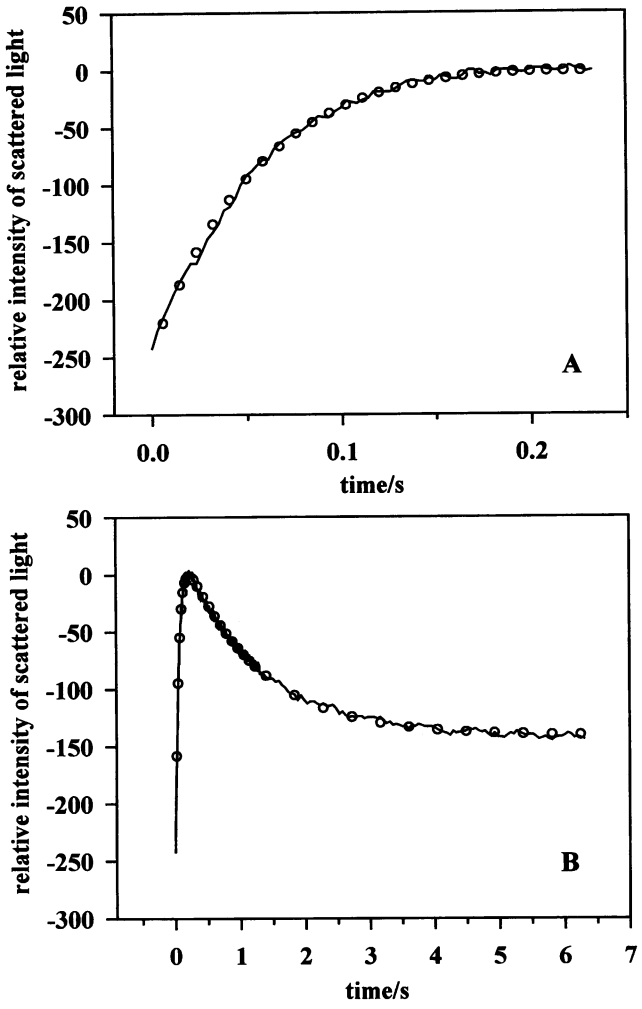

FIGURE 3 Time course of scattered light intensity upon dilution of dipalmitoleoyl-PC liposomes into hypertonic (200 mM glycerol) buffer on two different timescales. Buffers contained 50 mM K_2SO_4, 5 mM ACES, MES, TES, and Tricine each, pH 7. The symbols (○) show a fit of two exponentials with opposite signs to the data. (*a*) Rapid initial signal increase corresponding to liposome shrinkage caused by water efflux. (*b*) Slow signal recovery due to glycerol permeation into the liposomes.

V_w was the molar volume of water, V_o the internal volume of the vesicles, A the vesicular surface area, and Δc the osmotic gradient. The term A/V_o was substituted by $3/r$, using the mean hydrodynamic radius r of the liposomes. The permeability coefficients for the solutes were calculated from the rate constant of the second process, as demonstrated by Verkman (1985).

$$P_{solute} = kr/3 \quad (5)$$

RESULTS

Proton permeation

The proton permeability coefficients measured at a concentration gradient of 10^{-7} M were not affected by the direction of the pH jump. Results listed in Table 1 are the average of three to five repeats.

Fig. 4 displays a semilogarithmic plot of the proton permeability coefficient as a function of the thickness of the bilayer's hydrophobic region, *d*. The hydrophobic region is defined as twice the distance between the second and the last carbon atom of the fatty acid in the lipid. Values for *d* were measured by x-ray scattering for the longer species of lipids (Lewis and Engelman, 1983) and could be extrapolated by using a linear function for the shorter ones.

As revealed by Fig. 4, proton permeability coefficients strongly depend on membrane thickness, starting at a maximum value of $1.3 \cdot 10^{-2}$ cm/s for the shortest lipid and steadily decreasing to a value of $4.9 \cdot 10^{-5}$ cm/s for the longest lipid. It follows that proton permeability decreases by a factor of approximately 250 as the thickness of the hydrophobic region is increased from 20 Å to 37 Å. In addition, the slope of the curve in Fig. 4 is also a function of chain length. For example, the permeability decreases by a factor of approximately 7 between C14 and C16, but only by a factor of 1.5 between C22 and C24.

Potassium ion permeation

Fig. 5 shows potassium ion permeability coefficients as a function of bilayer thickness on a semilogarithmic scale. Observed permeabilities range between $1.5 \cdot 10^{-10}$ cm/s and $1.7 \cdot 10^{-12}$ cm/s. Compared to the other permeants, potassium ion gradients decay extremely slowly across phospholipid bilayers—seven to eight orders of magnitude slower than proton gradients and five to six orders of magnitude slower than urea or glycerol gradients (see following section).

Another important feature is the prominent biphasic nature of the curve. For the shortest three lipids, a steep drop

TABLE 1 Results of permeability measurements for protons, potassium ions, water, urea, and glycerol for six phosphatidylcholines of different chain length

d [Å]	log $P_{Protons}$	log $P_{Potassium}$	log P_{Water}	log P_{Urea}	log $P_{Glycerol}$
20.0	−1.89	−9.82	−1.61	−5.47	−5.21
23.5	−2.74	−11.03	−1.71	−5.61	−5.43
27.0	−3.29	−11.46	−1.82	−5.85	−5.56
30.5	−3.80	−11.62	−1.95	−5.97	−5.67
34.0	−4.10	−11.66	−2.15	−6.11	−5.88
37.5	−4.31	−11.77	−2.30	−6.22	−5.97

Permeabilities are in centimeters per second. *d* is the thickness of the hydrophobic region of the bilayer (Lewis and Engelman, 1983).

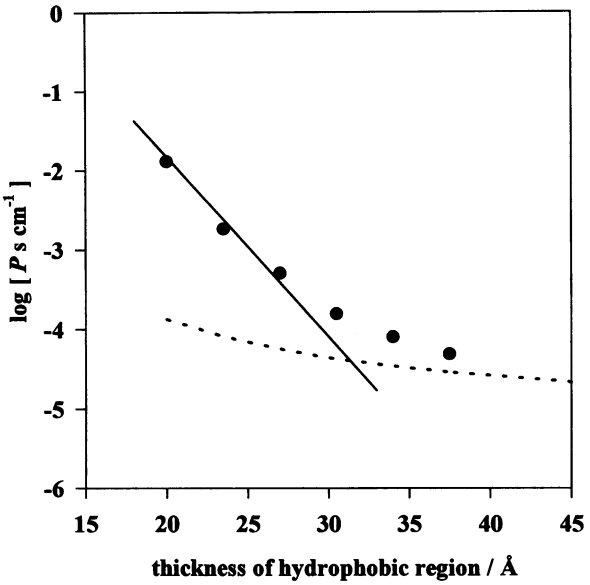

FIGURE 4 Dependence of proton permeability on membrane thickness d on a semilogarithmic scale. Points are experimental data, the solid line is calculated according to Eq. 15 (pore model), and the dotted line is calculated according to Eq. 6 (solubility-diffusion model). Parameters: $r(H_3O^+)$ = 1.1 Å, $r(H_9O_4^+)$ = 3.9 Å, ϵ_α = 78, ϵ_β = 2, $\gamma_{\alpha/\beta}$ = 30 mN m^{-1}, D = 1.4 · 10^{-4} cm^2 s^{-1}, σ = 10, R_v = 1.05 · 10^{-6} cm, A = 26 000 cm^{-1}, n_o = 1.04 · 10^{29} cm^5, T = 303.15 K, k_1 = 2.2 · 10^{15} kJ mol^{-1} cm^{-2}, k_2 = 9 · 10^7 kJ mol^{-1} cm^{-1}.

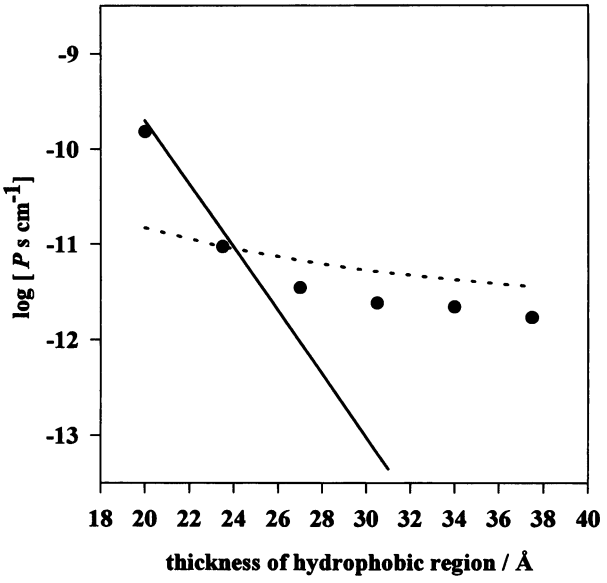

FIGURE 5 Dependence of potassium ion permeability on membrane thickness d on a semilogarithmic scale. Points are experimental data, solid line is calculated according to Eq. 15 (pore model), and the dotted line is calculated according to Eq. 6 (solubility-diffusion model). Parameters: $r(K^+)$ = 1.49 Å, $r(K^+$, hydrated) = 3.31 Å, ϵ_α = 78, ϵ_β = 2, $\gamma_{\alpha/\beta}$ = 30 mN m^{-1}, D = 2 · 10^{-5} cm^2 s^{-1}, σ = 10, R_v = 1.05 · 10^{-6} cm, A = 26 000 cm^{-1}, n_o = 1.04 · 10^{29} cm^5, T = 303.15 K, k_1 = 2.2 · 10^{15} kJ mol^{-1} cm^{-2}, k_2 = 1.9 · 10^8 kJ mol^{-1} cm^{-1}.

in permeability accompanies the reduction of bilayer thickness, lowering the value of the permeability coefficient from 1.5 · 10^{-10} to 3.5 · 10^{-12} cm/s. However, when the lipids are longer than 18 carbons per fatty acid, the curve levels off and displays only a moderate slope, which more closely resembles the patterns seen for water, glycerol, and urea (see following section and Fig. 6).

Water, glycerol, and urea permeation

Fig. 6 illustrates how the water permeability coefficient is affected by the thickness of the bilayer. Every data point represents the average result of five experimental trials (also see Table 1) for each solute. Although permeabilities become noticeably smaller with increasing bilayer thickness, the magnitude of this decrease is much smaller than that observed for protons. The permeability coefficient for the longest lipid (2.4 · 10^{-2} cm/s) is only about five times lower than for the shortest (5.0 · 10^{-3} cm/s). Furthermore, the slope of the curve is roughly constant, which is in sharp contrast to the biphasic behavior observed for potassium ions.

Glycerol and urea display quite similar permeabilities (see Fig. 6), with glycerol being slightly more permeable than urea. The values were in the range of 6.2 · 10^{-6} to 1.1 · 10^{-6} cm/s and 3.4 · 10^{-6} to 6.0 · 10^{-7} cm/s for glycerol and urea, respectively. This indicates that the membrane represents a significantly higher diffusion barrier to these molecules than to water or protons. The slope of the permeability coefficient plotted against bilayer thickness resembles that of water (see Fig. 6), with permeability values for the longest and shortest lipids differing by roughly fivefold.

DISCUSSION

Before discussing the effect of bilayer thickness on the permeability and possible permeation mechanisms, we will compare the values for permeability coefficients determined in this study to previously published data. Reported values for proton permeability coefficients vary over a wide range, from 10^{-2} cm/s to 10^{-7} cm/s (Nichols and Deamer, 1980; Nichols et al., 1980; Biegel and Gould, 1981; Elamrani and Blume, 1983; Grzesiek and Dencher, 1986; Perkins and Cafiso, 1986; Norris and Powell, 1990). This variation relates to the use of different techniques, lipids, and bilayer systems (liposomes and planar bilayers) or different pH ranges (Perkins and Cafiso, 1986). The proton data of this study agree with the higher reported values. Published permeability coefficients of phospholipid bilayers to potassium ions cover a broad spectrum, with reported values between 10^{-9} cm/s and 10^{-13} cm/s, depending on technique and type of lipid (Papahadjopoulos, 1971; Hauser et al., 1973; Barchfeld and Deamer, 1988; Hamilton and Kaler, 1990; Venema et al., 1993). The results of this study are consistent with the mid-range of these values. The osmotic permeability coefficients for water are somewhat higher than the values reported for related systems (Carruthers and Mel-

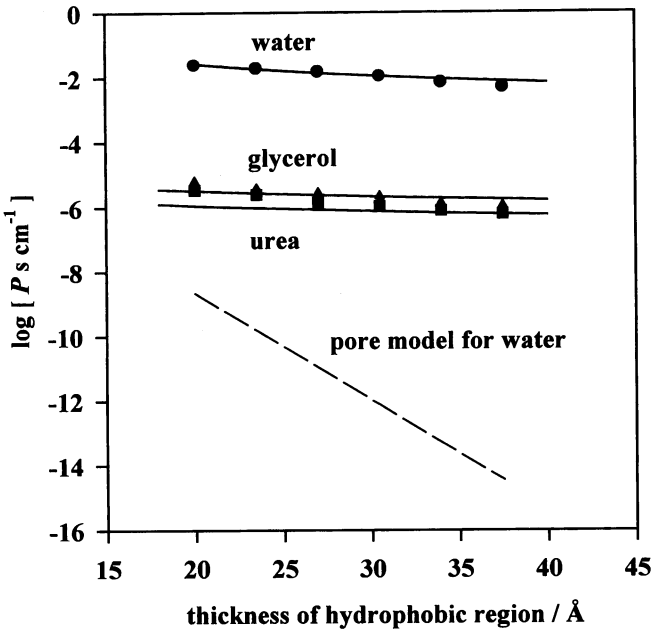

FIGURE 6 Dependence of water, urea, and glycerol permeability on membrane thickness d on a semilogarithmic scale. Points are experimental data, solid lines are calculated according to Eq. 6 for the solubility-diffusion model, and the dashed line is obtained from Eq. 15 (pore model, for water only). Parameters: r_{water} = 1.2 Å, r_{urea} = 2.8 Å, $r_{glycerol}$ = 2.9 Å, $\gamma_{\alpha/\beta}$ = 30 mN m^{-1}, p_{water} = 1.85 D, a_{water} = 1.38 Å, ΔG_{HB} (water) = 27 kJ mol^{-1}, ΔG_{HB} (urea/glycerol) = 3 · 21 kJ mol^{-1}, $D_{water} = 4.59 \cdot 10^{-5}$ cm^2 s^{-1}, $D_{urea} = 1.38 \cdot 10^{-5}$ cm^2 s^{-1}, $D_{glycerol} = 1.06 \cdot 10^{-5}$ cm^2 s^{-1}.

chior, 1983; Verkman et al., 1985; Lawaczeck, 1988; Ye and Verkman, 1989; Finkelstein, 1987; Priver et al., 1993; Jansen and Blume, 1995). A typical value for P_f in planar bilayers made from egg PC, which is quite similar to the lipids used here, is $3 \cdot 10^{-3}$ cm/s at 25°C (Finkelstein, 1987). The elevated temperature and the presence of double bonds in each lipid chain can account, at least in part, for the high P_f values we observed. Reported urea and glycerol permeability coefficients in phospholipid bilayers range between 10^{-6} cm/s and 10^{-7} cm/s (Verkman et al., 1985; Finkelstein, 1987; Priver et al., 1993), which is consistent with the observations of this study.

If the dependence of permeability on membrane thickness is analyzed, a clear difference between the ions and the uncharged molecules emerges. Semilogarithmic P versus d plots of the neutral species display slopes that remain essentially constant throughout the whole bilayer thickness range. This is in contrast with the data for protons and particularly for potassium ions, which exhibit a prominent biphasic pattern with steeper slopes observed for the shorter lipids. The curves level off at chain lengths longer than 16 to 18 carbon atoms for potassium ion permeation and 20 to 22 carbon atoms for proton permeation, so that slopes resemble those of the neutral molecules. For potassium ions, this change in slope takes place at a smaller d than for protons and is more abrupt. These observations can be interpreted in terms of the two alternative permeation mechanisms. To assign a specific permeation mechanism to a given slope, the predictions of both the solubility-diffusion and the pore model will be discussed. We will use two relatively simple models that permit the calculation of the permeability coefficient as a function of bilayer thickness.

The solubility-diffusion mechanism

This model depicts the bilayer membrane as a thin static slab of liquid hydrocarbon matter separating two aqueous phases. Permeating particles must partition into the hydrophobic region, diffuse across, and leave by re-dissolving into the second aqueous phase. In the simplest case, the permeability coefficient of a particle crossing a bilayer can be expressed as follows (Hauser et al., 1973; Markin and Kozlov, 1985; Finkelstein, 1987; Gennis, 1989):

$$P = KD/d, \tag{6}$$

where K is the partition coefficient of the permeating species between water and a liquid hydrocarbon resembling the hydrophobic membrane interior. D represents the diffusion coefficient of the permeating species inside the membrane. Because of the extremely low solubility of many ions and polar molecules in hydrocarbon solvents, D is unknown in most cases, with the exception of water, for which D has been measured in hydrocarbons (Schatzberg, 1965). As pointed out by Finkelstein, the diffusion coefficient of the permeating species in water can serve as a reasonable approximation for D (Finkelstein, 1987). The bilayer thickness is given as d, which equals the thickness of the hydrophobic region.

The critical parameter in Eq. 6 is the partition coefficient K, which can be calculated (Hauser et al., 1973; Markin and Volkov, 1989) from the Gibbs free energy (ΔG) required to transfer a particle from an aqueous to a hydrophobic phase, as follows:

$$K = \exp[-\Delta G/RT]. \tag{7}$$

In the case of ions that are not involved in chemical reactions or specific interactions with the solvent, ΔG can be expressed as the sum of electrostatic (ΔG_B and ΔG_I) and hydrophobic energies (ΔG_S):

$$\Delta G = \Delta G_B + \Delta G_I + \Delta G_S. \tag{8}$$

Two terms contribute to the electrostatic energy: the classical Born energy, ΔG_B (Born, 1920), and image energies, ΔG_I. The Born energy term takes into account the electrostatic energy required to move an ion of radius r from water (ϵ_w) into a hydrophobic environment with a low dielectric constant ϵ_{hc} , such as the interior of a bilayer (Parsegian, 1969; Dilger et al., 1979).

$$\Delta G_B = \frac{e^2 z^2}{8 \pi \epsilon_o r}(1/\epsilon_{hc} - 1/\epsilon_w) \tag{9}$$

Because the bilayer is assumed to be a thin slab of hydrophobic matter, image energies arising from interac-

tions of the penetrating particle with the water-membrane interfaces must be added to the Born energy term. As shown by Neumcke and Läuger, the following expression can be used to compute the image energy (Neumcke and Läuger, 1969) of an ion that is located at distance x normal to the membrane surface:

$$\Delta G_I = \frac{e^2 z^2 \vartheta}{8 \epsilon_{hc} d}\left[-\frac{d}{x} + S\left(\vartheta, \frac{r}{d}\right) - S\left(\vartheta, \frac{x}{d}\right) + \frac{1}{\vartheta^2} S\left(\vartheta, -\frac{r}{d}\right) - \frac{1}{\vartheta^2} S\left(\vartheta, -\frac{x}{d}\right)\right] \quad (10a)$$

$$S(\vartheta, r/d) = \sum_{v=1}^{\infty} \frac{\vartheta^{2v}}{v + r/d} \quad (10b)$$

$$\vartheta = \frac{\epsilon_w - \epsilon_{hc}}{\epsilon_w + \epsilon_{hc}}. \quad (10c)$$

In most instances, the contribution of image energy to the total energy is very small, unless the membrane is extremely thin.

Another substantial energy term is the hydrophobic (solvophobic, neutral) energy, ΔG_S, which is associated with the transfer of an uncharged particle of radius r from water into a hydrophobic phase. ΔG_S is well described by Uhlig's formula (Markin and Volkov, 1989). This approach uses the surface energy $\gamma_{\alpha/\beta}$ between an aqueous and a hydrocarbon phase to quantify ΔG_S (Eq. 11). Although derived for macroscopic applications, this equation has proved to be useful on the microscopic scale as well.

$$\Delta G_S = -N_a 4\pi r^2 \gamma_{\alpha/\beta} \quad (11)$$

The combination of Eqs. 9, 10, and 11 permits the calculation of the total Gibbs free energy of transfer and the partition coefficient K of an ion (Eq. 7). Inserting K into Eq. 6 gives permeability coefficients predicted by the solubility-diffusion mechanism. More importantly, it allows the calculation of P as a function of the bilayer thickness, d.

A critical parameter in all of the equations above is the ionic radius r, because P is extremely sensitive to minor changes in r. Depending on whether the bare or the hydrated ionic radius is used, the results for ΔG and inevitably for P differ significantly. If the bare radius is used, energies of transfer are so high that the obtained permeabilities are many orders of magnitude smaller than those observed in experiments. Therefore, only hydrated ionic radii (Conway, 1981) seem to be suitable parameters for permeability calculations based on the solubility-diffusion mechanism.

For the uncharged permeants water, urea, and glycerol, K can be obtained in a similar manner. ΔG can be written as the sum of electrostatic energies, hydrophobic energy, and the energy associated with the breakage of hydrogen bonds between the polar molecule and water (ΔG_{HB}):

$$\Delta G = \Delta G_B + \Delta G_I + \Delta G_S + \Delta G_{HB}. \quad (12)$$

Because the solutes do not carry a net charge, electrostatic interactions (Born energy and image energy) will contribute to ΔG only if the molecule is small and has a significant dipolar moment. This is only the case for water. The Born energy of transfer of a dipole from water into a hydrocarbon environment, $\Delta G_{B(dip)}$, has the form

$$\Delta G_{B(dip)} = \frac{p^2}{3a^3}\left(\frac{1}{\epsilon_{hc}} - \frac{1}{\epsilon_w}\right), \quad (13)$$

where p is the dipolar moment and a is the effective dipole size. For water, a dipolar moment of 1.85 D and an effective dipole size of 1.38 Å was used in the calculation (Arakelian and Arakelian, 1983). The contribution of image forces to the electrostatic energy term for a dipole was calculated according to the method of Arakelian and Arakelian (1983):

$$\Delta G_{I(dip)} = -\frac{2p^2}{3\epsilon_{hc} d^3} \sum_{i=1}^{\infty}\left(\frac{2\vartheta^{2i-1}}{(2i-1)^3}\right) \quad (14)$$

$$\vartheta = \frac{\epsilon_w - \epsilon_{hc}}{\epsilon_w + \epsilon_{hc}}. \quad (10c)$$

ΔG_{HB} was approximated by 27 kJ/mol for the breakage of a hydrogen bond between two water molecules and by 63 kJ/mol for hydrogen bonds between three water molecules and a glycerol or urea molecule, respectively (Pimentel and McClellan, 1960).

Overall, the permeability coefficients predicted by the solubility-diffusion mechanism display only a moderate dependence on membrane thickness. For uncharged permeating particles without a significant dipolar moment, a semilogarithmic plot of P against d should ideally give a straight line because in this case, neither D nor K depends on d. Only in the case of ions, small, strong dipoles, and very thin membranes will K be effected by the membrane thickness, and a small deviation from a straight line is expected. Nonetheless, the overall influence of d on P remains rather small.

The pore mechanism

The pore model suggests that permeation occurs through transient hydrated pores produced by thermal fluctuations within the bilayer (Nagle and Scott, 1978; Nichols and Deamer, 1980; Elamrani and Blume, 1983; Lawaczeck, 1988; Deamer and Nichols, 1989; Hamilton and Kaler, 1990; Ipsen et al., 1990; Jansen and Blume, 1995). By passing through such hydrated defects, the permeating particles can largely evade the high-energy barrier associated with partitioning into the hydrophobic membrane interior. For instance, Parsegian showed that the Born energy for a charged particle of radius 2 Å is reduced from 168 kJ/mol to 28 kJ/mol if it passes a membrane of thickness 70 Å through a hydrated pore instead of partitioning into the hydrocarbon phase (Parsegian, 1969).

Computing the permeability predicted by the pore model is a complex mathematical task (Markin and Kozlov, 1985). An attempt to express the permeability in terms of a few elementary parameters, such as pore radius and pore depth, was undertaken by Hamilton and Kaler (1990). These authors determined cation permeabilities by measuring the escape rates of alkali ions from vesicles made from synthetic surfactants. They explained their results in terms of a pore model that considered only hydrophilic pores, meaning that the pore walls were lined with the polar (hydrated) headgroups of the lipid. The formation of hydrophobic pores was considered to be too costly energetically and thus unlikely. The probability of pore formation was expressed in terms of an exponential factor containing the energy required for pore formation. It was further postulated that this energy could be separated into two independent terms, one depending only on pore area and the other one depending only on pore depth. The permeability coefficient was expressed as

$$P = \frac{D_M \gamma n_o RT}{R_v A k_1}\left[\pi r^2 + \frac{RT}{k_1}\right]\exp\left[\frac{-k_1 \pi r^2}{RT}\right]\exp\left[\frac{-k_2 d}{RT}\right], \quad (15)$$

where D_M is the diffusion coefficient of the permeating particle in water; γ is the surface concentration enhancement factor due to the effect of the electric double layer; A is the membrane surface; R_v is the radius of the vesicles; R is the gas constant; T is the temperature; n_o is the maximum pore number; r is the pore radius; and d is the pore depth. The constants k_1 and k_2 refer to the energy associated with the formation of a pore of radius r and depth d, respectively. Because only pores that completely span the membrane allow permeation to take place, the pore depth necessarily equals the thickness of the membrane. As a result, Eq. 15 can be used to calculate P as a function of membrane thickness d.

An important issue that has implications for the magnitude of k_1 and k_2 is whether to use the hydrated or bare radius of the penetrating particle. Hamilton and Kaler indicated that the hydration shell of ions is likely to be replaced by water molecules of hydrated headgroups when passing the pore, assuming a 2.8 Å hydration layer around the lipid headgroups. This implies that the bare ionic radius together with an increment for the hydration layer must be used in Eq. 15 .

Hamilton and Kaler determined the constants k_1 and k_2 by fitting Eq. 15 to their set of experimental data points. As an alternative, the energy of pore formation can also be calculated by using splay and saddle splay bending constants of the membrane (Frank, 1958). These bending constants are known for egg phosphatidylcholine. Although the surfactants used by Hamilton and Kaler were different from phosphatidylcholines, they computed energies of pore formation from the fitted values of k_1 and k_2, which were in good agreement with those calculated from the bending constants for egg phosphatidylcholine (Hamilton and Kaler, 1990).

k_2 is the parameter that determines the slope of a semilogarithmic plot of P versus d. Using Hamilton and Kaler's k_2 value, the slope predicted by this simplified pore model is much steeper than the slope predicted by the solubility-diffusion model. Thus, the membrane thickness dependence of P can indicate which mechanism is dominant for a specific permeating particle in a given system.

Application of the models to the results

The assignment of a permeation mechanism based on the dependence of P on d is easiest for the uncharged permeants water, urea, and glycerol. Here, the moderate dependence of P on d is consistent with a solubility-diffusion mechanism for these molecules. Using the calculated partition coefficients, the diffusion coefficient of water in a hydrocarbon phase, and the diffusion coefficients of urea and glycerol in water, reasonable fits to the data points can be achieved (see Fig. 6). Although slightly lower than the experimental points, the calculated permeabilities are the right order of magnitude. In addition, the slopes of calculated P versus d plots are similar to the experimental slopes, although for urea and glycerol they are slightly smaller. Analogous calculations for neutral permeants based on the pore mechanism show two inconsistencies (Fig. 6 illustrates this for water). First, the computed permeabilities are too low by orders of magnitude. Second, the dependence of P on bilayer thickness is not properly described. These findings suggest that permeation of uncharged polar molecules is more appropriately characterized by solubility-diffusion than by the pore formation. The contribution of pores to the net permeability seems to be negligible.

Additional support for a solubility-diffusion mechanism for water was provided by Finkelstein, who measured the diffusional and osmotic water permeability (P_d and P_f) of planar lipid bilayers (Finkelstein, 1987). The observation that these two quantities were equal contradicted an involvement of a single-file pore mechanism in water permeation. These findings were confirmed by Ye and Verkman, who determined P_d and P_f simultaneously in phospholipid liposomes by optical methods and reported a P_f/P_d ratio of 1 (Ye and Verkman, 1989).

Using calculations based on literature values, Markin and Kozlov ruled out the involvement of pores in permeation of uncharged particles across a membrane (Markin and Kozlov, 1985). Permeabilities obtained from pore statistics gave values that were markedly lower than experimental observations, in agreement with the data presented in Fig. 6. Overall, the solubility-diffusion mechanism seems to impose a significantly lower permeation barrier on neutral molecules than the pore mechanism and is therefore the more likely permeation mechanism for these molecules.

In contrast, Jansen and Blume recently presented evidence that water permeation of liposomes occurs predominantly through defects, rather than by solubility-diffusion (Jansen and Blume, 1995). Their approach was to measure

the P_f/P_d ratio for water permeation in liposomes containing saturated lipid chains from 14 to 18 carbon atoms in length, both above and below the phase transition temperature, T_m. The results showed that P_f/P_d was larger than 1, with values of 60, 5, and 35 below T_m, and 7, 7, and 24 above T_m for 14, 16, and 18 carbon atoms. Based on this observation, the authors concluded that water permeation occurs primarily by pore formation, rather than by solubility and diffusion. Our evidence suggests that ion-conducting defects begin to appear as chain length decreases below 18 carbons but are too rare to provide a major pathway for water permeation.

Before discussing this further, we should indicate differences in experimental conditions between the two investigations. First, we used lipids that were monounsaturated in both chains, whereas Jansen and Blume used saturated lipids. Second, the osmotic gradient in our study was inward, created by permeant solutes, so that the liposomes first underwent a modest decrease in volume, followed by a volume increase as solutes penetrated the lipid bilayers. Jansen and Blume applied an outward gradient by diluting liposomes prepared in 100 mM glucose to a final glucose concentration of 50 mM, so that osmotic swelling occurred. Furthermore, Jansen and Blume observed no obvious relationship between chain length and water permeability, whereas we observed an approximately linear dependence on chain length, so that water permeability was reduced about fivefold, as chain length was increased from 14 to 24 carbon atoms.

The experimental conditions used by the two investigations are sufficiently different so that no immediate conclusions can be drawn. Probably the most significant difference concerns saturated and unsaturated lipid chains. Saturated lipids may in fact conduct water largely through defects, and unsaturated lipids largely by a solubility-diffusion process, a conjecture that is supported by the relatively high water permeability observed in unsaturated liposomes. In future studies it will be interesting to compare P_f/P_d in liposomes composed of saturated and unsaturated lipids.

In contrast to the uncharged permeants, the data indicate that a combination of both mechanisms is responsible for ion permeation. For potassium ion permeation, the solubility-diffusion mechanism can properly describe P only for the longer lipids, provided that the permeating species is a hydrated potassium ion of radius 3.31 Å. If the number of carbon atoms in the lipid acyl chain is less than 18, the solubility-diffusion model fails to describe the experimental data accurately, because the computed values and the slope of a P versus d graph are both too small. In this region, permeation through pores describes the experimental evidence more properly. Equation 15 and the k_2 parameter provided by Hamilton and Kaler give reasonable fits to the data points, as depicted in Fig. 5. Apparently there is a transition from one permeation mechanism to the other in the chain length region between 16 and 18 carbons. It follows that the net permeability of a bilayer can be considered to be the sum of two individual permeabilities, in which the dominating permeation mechanism will account for the majority of the actual value of P and will dictate the slope of a curve obtained from plotting permeability against bilayer thickness.

Calculation of the proton permeability according to the pore model requires the knowledge of the particle radius and the diffusion coefficient. If protons are translocated through transient pores along water wires by a Grotthus-type mechanism, the use of a smaller k_2 value than in the case of metal ions is mandatory ($9 \cdot 10^7$ kJ mol^{-1} cm^{-1} instead of $1.9 \cdot 10^8$ kJ mol^{-1} cm^{-1}; Deamer and Volkov 1995). Provided the permeating species is a H_3O^+ ion of radius 1.1 Å, the pore model produces a good fit to the experimental data for the short and intermediate lipids (Fig. 4), and the slope of the curve matches the experimental data reasonably well. The fit was less satisfactory for the long lipids. Here, the solubility-diffusion mechanism produces acceptable results, but only if the permeating species is $H_9O_4^+$, a species known to exist in aqueous solutions. It is remarkable that the relatively small difference in radius between the otherwise very similar $H_9O_4^+$ (3.9 Å) ion and the hydrated potassium ion (3.31 Å) produces a difference in P of several orders of magnitude. The transition from the pore to the solubility-diffusion mechanism is located at some point between chain lengths of 20 and 22 carbons.

SUMMARY

In conclusion, pores seem to be the dominant permeation mechanism for ions, but only if the membrane is sufficiently thin. Ion permeation by partitioning and diffusion seems to become of greater importance as membrane thickness increases, because the number of pores in the membrane produced by thermal fluctuations certainly decreases as the bilayers become increasingly stable. This transition from one mechanism to another is observed at chain lengths between 16 and 18 carbons for potassium ions and at chain lengths between 20 and 22 carbons for protons. On the other hand, because of their high solubility in a hydrocarbon phase, neutral molecules apparently cross exclusively by the solubility-diffusion mechanism, regardless of membrane thickness.

We demonstrated that the experimental data can be described remarkably well by simple models, such as a continuum model for the solubility-diffusion mechanism and a semiempirical model for permeation through pores. Both models, however, neglect molecular details and the inhomogeneity of the bilayer. In this respect, molecular dynamics simulations are promising and perhaps are a more satisfying alternative (Egberts et al., 1994). For instance, the diffusion of water through a phospholipid membrane has been simulated, producing values for the permeability coefficient that are in agreement with experimental data (Marrink and Berendsen, 1994). It will be interesting to test the potential of this approach in the future.

We wish to thank Dr. A. S. Verkman for his advice and for making available his stopped-flow apparatus.

This work was supported by NASA grant NAGW-1119.

REFERENCES

Ames, B. N. 1966. Assay of inorganic phosphate, total phosphate and phosphatases. *Methods Enzymol.* 8:115–118.

Arakelian, V. B., and S. B. Arakelian. 1983. Energetic profile of a dipole molecule in the thin membrane. *Biol. J. Armenia.* 36:775–779.

Barchfeld, G. L., and D. W. Deamer. 1988. Alcohol effects on lipid bilayer permeability to protons and potassium: relation to the action of general anesthetics. *Biochim. Biophys. Acta.* 944:40–48.

Born, M. 1920. Volumen und Hydrationswärme der Ionen. *Z. Phys.* 1:45–48.

Carruthers A., and D. L. Melchior. Studies of the relationship between bilayer water permeability, and bilayer physical state. 1983. *Biochemistry.* 22:5797–5807.

Clement, N. R., and J. M. Gould. 1981. Pyranine (8-hydroxyl-1,3,6-pyrenetrisulfonate) as a probe of internal aqueous hydrogen ion concentration in phospholipid vesicles. *Biochemistry.* 20:1534–1538.

Cohen, B. E., and A. D. Bangham. 1971. Diffusion of small non-electrolytes across liposome membranes. *Nature.* 236:173–174.

Conway, B. E. 1981. Ionic Hydration in Chemistry and Biophysics. Elsevier, New York.

Deamer, D. W., and J. W. Nichols. 1989. Proton flux mechanisms in model and biological membranes. *J. Membr. Biol.* 107:91–103.

Deamer, D. W., and A. G. Volkov. 1995. Proton permeation of lipid bilayers. *In* Permeability and Stability of Lipid Bilayers. E. A. Disalvo and S. A. Simon, editors. CRC Press, Boca Raton, FL. 161–177.

De Gier, J. 1993. Osmotic behaviour and permeability properties of liposomes. *Chem. Phys. Lipids.* 64:187–196.

Dilger, J. P., S. G. A. McLaughlin, T. J. McIntosh, and S. A. Simon. 1979. The dielectric constant of phospholipid bilayers and the permeability of membranes to ions. *Science.* 206:1196–1198.

Egberts, E., S. J. Marrink, and H. J. C. Berendsen. 1994. Molecular dynamics simulation of a phospholipid membrane. *Eur. Biophys. J.* 22:423–436.

Elamrani, K., and A. Blume. 1983. Effect of the lipid phase transition on the kinetics of H^+/OH^- diffusion across phosphatidic acid bilayers. *Biochim. Biophys. Acta.* 727:22–30.

Finkelstein A. 1987. Water Movement Through Lipid Bilayers, Pores, and Plasma Membranes: Theory and Reality. Wiley Interscience, New York.

Frank, C. F. 1958. On the theory of liquid crystals. *Discuss. Faraday Soc.* 25:19–28.

Gennis, R. B. 1989. Biomembranes: Molecular Structure and Function. Springer Verlag, New York. 241–247.

Grzesiek, S., and N. A. Dencher. 1986. Dependency of ΔpH relaxation across vesicular membranes on the buffering power of bulk solutions and lipids. *Biophys. J.* 50:265–276.

Hamilton, R. T., and E. W. Kaler. 1990a. Alkali metal ion transport through thin bilayers. *J. Phys. Chem.* 94:2560–2566.

Hamilton, R. T., and E. W. Kaler. 1990b. Facilitated ion transport through thin bilayers. *J. Membr. Sci.* 54:259–269.

Hauser, H., D. Oldani, and M. C. Phillips. 1973. Mechanism of ion escape from phosphatidylcholine and phosphatidylserine single bilayer vesicles. *Biochemistry.* 12:4507–4517.

Ipsen, J. H., K. Jørgensen, and O. G. Mouritsen. 1990. Density fluctuations in saturated phospholipid bilayers increase as the acyl-chain length decreases. *Biophys. J.* 58:1099–1107.

Jansen, M., and A. Blume. 1995. A comparative study of diffusive and osmotic water permeation across bilayers composed of phospholipids with different head groups and fatty acyl chains. *Biophys. J.* 68: 997–1008.

Lawaczeck, R. 1988. Defect structures in membranes: routes for permeation of small molecules. *Ber. Bunsenges. Phys. Chem.* 92:961–963.

Lewis, B. A., and D. M. Engelman. 1983. Lipid bilayer thickness varies linearly with acyl chain length in fluid phosphatidylcholine vesicles. *J. Mol. Biol.* 166:211–217.

Markin, V. S., and M. M. Kozlov. 1985. Pore statistics in bilayer lipid membranes. *Biol. Membr.* 2:404–442.

Markin, V. S., and A. G. Volkov. 1989. The Gibbs free energy of ion transfer between two immiscible liquids. *Electrochim. Acta.* 34:93–107.

Marrink, S. J., and H. J. C. Berendsen. 1994. Simulation of water transport through a lipid membrane. *J. Phys. Chem.* 98:4155–4168.

Nagle, J. F., and H. L. Scott. 1978. Lateral compressibility of lipid mono- and bilayers. Theory of membrane permeability. *Biochim. Biophys. Acta.* 513:236–243.

Neumcke, B., and P. Läuger. 1969. Nonlinear electrical effects in lipid bilayer membranes. II. *Biophys. J.* 9:1160–1969.

Nichols, J. W., and D. W. Deamer. 1980. Net proton-hydroxyl permeability of large unilamellar liposomes measured by an acid-base titration technique. *Proc. Natl. Acad. Sci. USA.* 77:2038–2042.

Nichols, J. W., M. W. Hill, A. D. Bangham, and D. W. Deamer. 1980. Measurement of net proton-hydroxyl permeability of large unilamellar liposomes with the fluorescent pH probe, 9-aminoacridine. *Biochim. Biophys. Acta.* 596:393–403.

Norris, F. A., and G. L. Powell. 1990. The apparent permeability coefficient for proton flux through phosphatidylcholine vesicles is dependent on the direction of flux. *Biochim. Biophys. Acta.* 1030:165–171.

Papahadjopoulos, D. 1971. Na^+-K^+ discrimination by "pure" phospholipid membranes. *Biochim. Biophys. Acta.* 241:254–259.

Parsegian, A. 1969. Energy of an ion crossing a low dielectric membrane: solutions to four relevant electrostatic problems. *Nature.* 221:844–846.

Perkins, W. R., and D. S. Cafiso. 1986. An electrical and structural characterization of H^+/OH^- currents in phospholipid vesicles. *Biochemistry.* 25:2270–2276.

Pimentel, G. C., and McClellan, A. L. 1960. The Hydrogen Bond. Freeman, San Francisco.

Priver, N. A., E. C. Rabon, and M. L. Zeidel. 1993. Apical membrane of the gastric parietal cell: water, proton, and nonelectrolyte permeabilities. *Biochemistry.* 32:2459–2468.

Schatzberg, P. 1965. Diffusion of water through hydrocarbon liquids. *J. Polym. Sci. (C).* 10:87–92.

Small, D. M. 1967. Phase equilibria and structure of dry and hydrated egg lecithin. *J. Lipid Res.* 8:551–557.

Van Heeswijk, M. P. E., and C. H. van Os. 1986. Osmotic water permeabilities of brush border and basolateral membrane vesicles from rat renal cortex and small intestine *J. Membr. Biol.* 92:183–193.

Venema, K., R. Gibrat, J. P. Grouzis, and C. Grignon. 1993. Quantitative measurement of cationic fluxes, selectivity and membrane potential using liposomes multilabeled with fluorescent probes. *Biochim. Biophys. Acta.* 1146:87–96.

Verkman, A. S., J. A. Dix, and J. L. Seifter. 1985. Water and urea transport in renal microvillus membrane vesicles. *Am. J. Physiol.* 650–655.

Ye, R., and A. S. Verkman. 1989. Simultaneous optical measurement of osmotic and diffusional water permeability in cells and liposomes. *Biochemistry.* 28:824–829.